Verification of Constructive Solid Geometry Modeling in GPU-Optimized Reactor Physics Monte Carlo Code, GREAPMC

Hyungwoo Sohn[a], Murat Serdar Aygul[a], Deokjung Lee[a*]
[a]*Department of Nuclear Engineering, Ulsan National Institute of Science and Technology, 50 UNIST-gil, Ulsan, 44919, Republic of Korea*
*Corresponding author: deokjung@unist.ac.kr

***Keywords : GPU, Monte Carlo, GREAPMC, VERA**

1. Introduction

The CORE research group at Ulsan National Institutes of Science and Technology (UNIST) has developed a GPU-optimized REActor Physics Monte Carlo code, GREAPMC [1]. To maximize computational performance, GREAPMC adopted a predefined cell-based geometry modeling approach rather than the Constructive Solid Geometry (CSG) method commonly employed in Monte Carlo codes. In the cell-based modeling, a cell containing the particle is known during the transport loop, avoiding additional cell-search operations. Despite its computational advantages, the cell-based modeling has limitation in representing complex three-dimensional (3D) geometries, particularly ex-core structures and detailed reactor components. To improve modeling flexibility and extend applicability to more general reactor configurations, a CSG capability has been implemented in GREAPMC.

2. Benchmark Specification

For verification of the CSG capability, the VERA Core Physics Benchmark [2], which is based on the Watts Bar Nuclear 1 (WBN1), a Westinghouse-designed 17x17 pressurized water reactor (PWR) was modeled and solved using the CSG capability implemented in GREAPMC. Progression problems 1-4 and a single case of Problem 5 were compared against reference solutions. These span geometries ranging from a two-dimensional (2D) single fuel pin cell to a 3D whole core configuration without thermal-hydraulic (TH) feedback or depletion.

KENO-VI results from the VERA benchmark specification were used as the reference, and GREAPMC results were additionally compared with MCS calculations in [3] for cross-code consistency.

Table I: The VERA benchmark progression problem 1-5

No.	Description
1	2D HZP BOC Pin Cell
2	2D HZP BOC Fuel Assembly
3	3D HZP BOC Fuel Assembly
4	2D, 3D HZP BOC 3×3 Fuel Assembly CRD Worth
5	Physical Reactor Zero Power Physics Tests (ZPPT)

3. Numerical Results

The ENDF/B-VII.0 library was adopted because both the benchmark document and the MCS results were generated using this library. For GREAPMC simulations, statistical uncertainties of the eigenvalue (k_{eff}) were maintained below 4 pcm, while the relative statistical uncertainties of tally were controlled within 1.5 %.

3.1. VERA Core physics problem 1

The first problem accesses GREAPMC's capability to solve a simple 2D pin cell eigenvalue problem. A single Westinghouse 17×17-type fuel pin-cell problems, consisting of UO_2, Zircaloy-4 cladding and water moderator under typical operating conditions were solved. Fuel and moderator temperature (T_F, T_M) and density(ρ_M) conditions are listed in Table II.

Table II: Temperatures and densities for problem 1

No.	T_F (K)	T_M (K)	ρ_M (g/cc)
1A	565	565	0.743
1B	600	600	0.661
1C	900	600	0.661
1D	1200	600	0.661
1E	600	600	0.743

Table III summarizes the calculated eigenvalues and differences relative to the references. For all cases in problem 1, the differences relative to MCS remain within 15 pcm, demonstrating accurate implementation of the CSG modeling for simple geometries. Slightly larger deviation observed with respect to KENO-VI may be attributed to differences in calculation options, which are not fully documented in the benchmark document.

Table III: Problem 1 solutions by GREAPMC

No.	Integral Absorber	k_{eff} (±3pcm)	Difference (pcm)	
		GREAPMC	MCS	KENO-VI
1A	NONE	1.18699	-14	-5
1B	NONE	1.18174	-9	-41
1C	NONE	1.17161	-10	-11
1D	NONE	1.16311	-15	51
1E	IFBA	0.77116	6	-53

3.2. VERA Core physics problem 2

The second problem evaluates the capability to model a 2D fuel assembly (FA). Various neutron poisons and integral burnable absorbers including silver-indium-cadmium (AIC), boron carbide (B_4C), pyrex, B_4C-Al_2O_3, IFBA and gadolinia are inserted into the guide tubes. Operating conditions are listed in Table IV.

Table IV: Temperatures and densities for problem 2

No.	T_F (K)	T_M (K)	ρ_M (g/cc)
2A	565	565	0.743
2B	600	600	0.661
2C	900	600	0.661
2D	1200	600	0.661
2E – 2P	600	600	0.743

Table V summarizes the eigenvalues obtained by GREAPMC. Eigenvalue differences between GREAPMC and MCS remains within approximately 13 pcm, indicating consistent CSG modeling for various discrete and integral absorbers. Larger deviation observed in comparison with KENO-VI may be attributed to differences in detail calculation options.

Table V: Problem 1 solutions by GREAPMC

No.	Poison	k_{eff}(±3pcm)	Difference (pcm)	
		GREAPMC	MCS	KENO-VI
2A	No poison	1.18231	-13	13
2B	No poison	1.18293	-6	-43
2C	No poison	1.17392	-9	17
2D	No poison	1.16578	-10	19
2E	12Pyrex	1.06917	-7	-46
2F	24Pyrex	0.97530	-9	-72
2G	24AIC	0.84677	-11	-92
2H	24B4C	0.78718	-8	-104
2I	IT	1.17951	-2	-41
2J	IT + 24Pyrex	0.97455	-8	-64
2K	Zoned + 24Pyrex	1.01936	-11	-70
2L	80 IFBA	1.01841	-13	-50
2M	128 IFBA	0.93825	-9	-55
2N	124IFBA 20WABA	0.86900	-13	-62
2O	12 Gadolinia	1.04729	-4	-44
2P	24 Gadolinia	0.92692	-6	-49

3.3. VERA Core physics problem 3

The third problem evaluates capability to model a 3D FA including non-fuel structures such as spacer grid, plenum, core plates and nozzles. This problem accesses the accuracy of CSG modeling for axial heterogeneities and non-fuel structural materials located above and below the fuel stack, as well as the impact of spacer grids on neutron flux and power distributions. The operating conditions are summarized in Table VI.

Table VI: Fuel and moderator condition for problem 3

No.	Enrichment (%)	T_M (K)	ρ_M (g/cc)	Boron (ppm)
3A	3.100	600	0.743	1300
3B	2.619	565	0.743	1066

Eigenvalue differences relative to MCS remain within 8 pcm, confirming accurate 3D modeling. Slightly larger deviations are observed compared with KENO-VI, consistent with earlier problems. Power distributions (Fig. 1, 2 and 3) also show good agreement. For case 3A, the RMS pin power error relative to KENO-VI is 0.18 % while case 3B is 0.07 %. These indicate that the implemented CSG capability reproduces detailed power distributions, including axial structural heterogeneities.

Table VII: Problem 3 solutions by GREAPMC

No.	Poison	k_{eff}(±3pcm)	Difference (pcm)	
		GREAPMC	MCS	KENO-VI
3A	No poison	1.17539	-8	-33
3B	16 Pyrex	0.99977	-5	-38

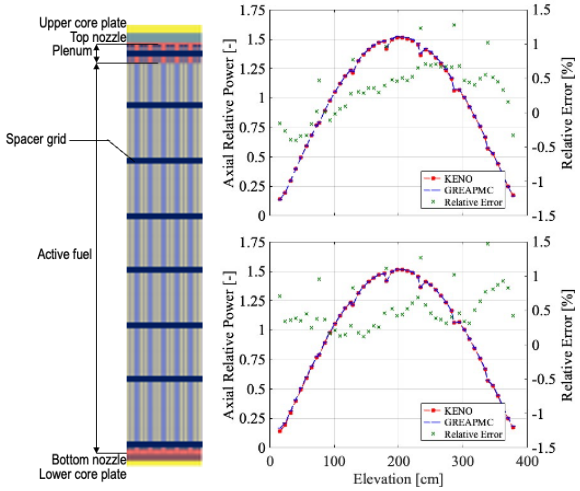

Fig. 1. Axial geometry of 3D FA(left) and axial power distribution of 3A (top) and 3B (bottom)

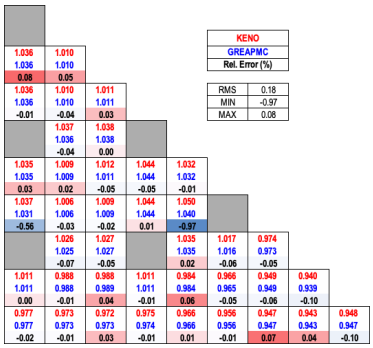

Fig. 2. Radial power distribution of 3A

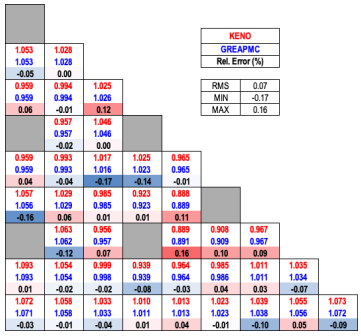

Fig. 3. Radial power distribution of 3B

3.4. VERA Core physics problem 4

The fourth problem evaluates the capabilities to predict eigenvalue, pin power distribution and control rod worth in the presence of neutron absorber. Configuration of this problem consists of FAs arranged in a 3x3 checkerboard pattern with rod cluster control assemblies (RCCAs) inserted in the central assembly under BOC hot zero power (HZP) isothermal conditions

(T_M of 565K and boron concentration of 1300 ppm). Control rod worth is evaluated by varying the hybrid AIC/B_4C RCCAs insertion depth. A reference rod position is defined at discrete elevation of 257.9cm from the bottom core plate. At this position, both pin-wise power distributions and axial power distributions are analyzed to assess the spatial accuracy of the implemented CSG modeling.

Prior to solve the 3D configurations, 2D cases at same operating conditions were solved. Table VIII and IX summarizes the eigenvalue and control rod worth for the 2D cases. Eigenvalue differences relative to MCS remain within 12 pcm for all configurations, indicating accurate treatment of absorber material. Control rod worth predictions also show good agreement with MCS, with differences within 5 pcm. Fig. 4 shows the pin-wise distributions and corresponding relative errors with respect to KENO-VI. The RMS errors are 0.11%, 0.14% and 0.13% respectively. Maximum deviations remain 0.80 % in magnitude for all cases. These results confirm accurate modeling of absorber configurations.

Table VIII: Problem 4-2D solutions (k_{eff}) by GREAPMC

No.	Description	k_{eff}(±3pcm)	Difference(pcm)	
		GREAPMC	MCS	KENO-VI
4A2D	Uncontrolled	1.00984	-10	-39
4B2D	AIC Controlled	0.98300	-12	-45
4C2D	B4C Controlled	0.97978	-5	-51

Table IX: Problem 4-2D solutions(rod worth) by GREAPMC

No.	Description	Rod worth	Difference	
		GREAPMC	MCS	KENO-VI
4B2D	AIC Controlled	-2703	-2	-7
4C2D	B4C Controlled	-3038	-5	-13

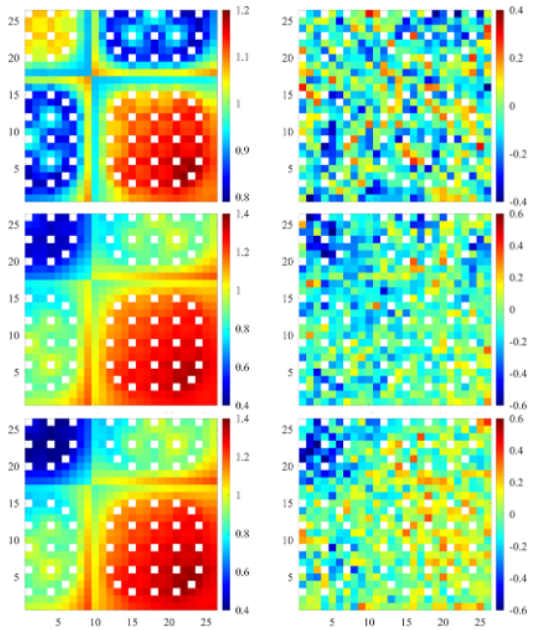

Fig. 4. Pin-wise power distribution and corresponding relative errors (%) relative to KENO-VI of 4A3D (top), 4B2D (middle) and 4C2D (bottom)

Table X summarizes the eigenvalues of the 3D case of the problem 4. Differences relative to MCS remain within 16 pcm for all insertion positions. Fig. 5 and 6 present the radial pin-wise and axial power distribution with statistical uncertainty and relative difference at the reference RCCA position. The predicted power profile shows very good agreement with the reference solution, and the statistical uncertainty remains below 0.2%, indicating sufficient particle histories and reliable Monte Carlo convergence. The rod worth curves shown in Fig. 7 also exhibit consistent agreement with the reference results, confirming accurate prediction of control rod reactivity and overall spatial modeling performance.

Table X: Problem 4 solutions by GREAPMC

RCCA Withdrawn (%)	k_{eff}(±3pcm)	Difference (pcm)	
	GREAPMC	MCS	KENO-VI
0	0.97201	-6	-40
10	0.97328	-13	-40
20	0.97884	-15	-52
30	0.98662	-15	-42
40	0.99195	-7	-39
50	0.99539	-9	-35
60	0.99760	-11	-43
70	0.99915	-15	-40
80	1.00016	-15	-42
90	1.00086	-5	-31
100	1.00098	-15	-41
Reference RCCA position	0.99859	-16	-39

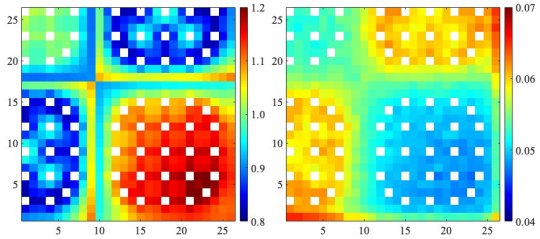

Fig. 5. Pin-wise power distribution and statistical uncertainty (%) of tally at reference RCCA position (problem 4 3D case)

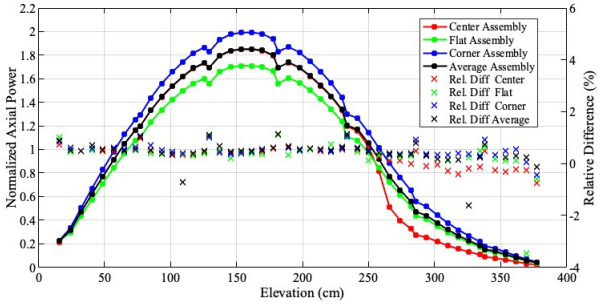

Fig. 6. Axial power distribution and relative error (%) at reference RCCA position (problem 4 3D case)

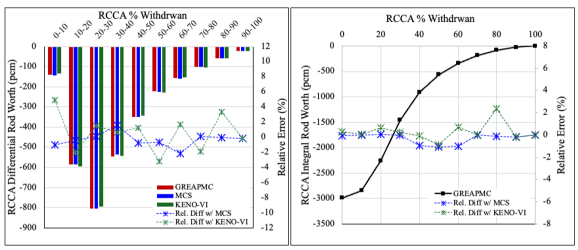

Fig. 7. RCCA differential rod worth (left) and integral rod worth (right) with relative differences

3.5. VERA Core physics problem 5

The fifth problem involves solving the ZPPT in a 3D whole core configuration of the WBN1 initial loading pattern, including ex-core structures. Power distributions under the HZP condition are evaluated. Although this problem includes criticality calculations and control rod worth evaluations for various bank position, the present study focuses on the reference case of Bank D at 167 steps withdrawn. The calculated eigenvalue is 0.99995 (±3 pcm). The difference relative to MCS and KENO-VI is 5 pcm and 23 pcm, respectively. The radial assembly power distribution also shows good agreement with the reference, with an RMS relative error of 0.21 % and deviations ranging from −0.36 % to 0.13 %, as shown in Fig 8. Fig 9 presents the normalized pin-wise power distribution with statistical uncertainty, which confirms consistent spatial agreement with the reference solution.

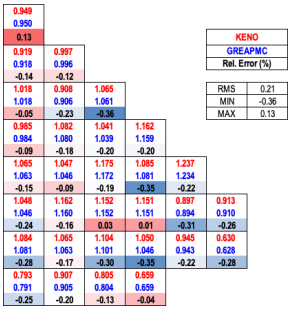

Fig. 8. Radial assembly power distribution and relative difference (%) of the problem 5 reference case

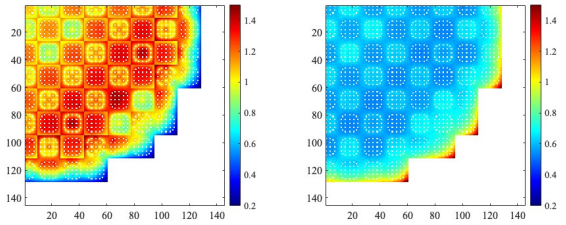

Fig. 9. Pin-wise power distribution and statistical uncertainty (%) of tally at reference RCCA position (problem 5)

3.6. Performance Comparison

Tracking rates are compared to evaluate the performance of the CSG capability in GREAPMC. A single NVIDIA RTX 3090 GPU is used for GREAPMC, while MCS is executed using 100 processes on three computational nodes with Intel Xeon Gold 6242R CPU.

Table XI summarizes the tracking rates from a 2D pin cell to 3D 3×3 FAs. The performance follows the order of cell based GREAPMC, CSG GREAPMC, and MCS, and decreases as the problem size increases. In the cell-based modeling, performance degradation is relatively small since particle locations are directly tracked by simple arithmetic operation of cell indices. In contrast, CSG modeling requires cell search operations through hierarchical geometry, making its performance more sensitive to the number of cells. This explains why performance degradation is more pronounced in CSG modeling than in the cell-based approach.

For 2D cases, the CSG GREAPMC shows performance comparable to MCS using about 200 CPU cores with a single GPU, while in 3D cases it corresponds to about 120 cores. MCS employs optimizations in cell search operation, such as neighbor cell lists, whereas the current CSG implementation in GREAPMC relies on exhaustive search through the entire hierarchical level. This indicates that the performance degradation in 3D cases of CSG GREAPMC is mainly due to the lack of optimized search, and further improvements can be achieved through algorithmic optimization.

Table XI: Comparison of tracking rates (10^3/s) for MCS, GREAPMC with CSG and cell-based modeling.

Problem No.	MCS (CSG)	GREAPMC (CSG)	GREAPMC (cell-based)
1B	286.9	544.9	1,302.0
2P	273.8	516.2	1,412.9
3B	127.9	150.0	1,113.7
4 – ref	122.6	153.0	1,121.6

4. Conclusion and Future Works

The implemented CSG capability in GREAPMC was verified using the VERA Benchmark progression problems, demonstrating accurate predictions of eigenvalue, power distribution, and control rod worth across both 2D and 3D configurations. These results confirm that the CSG modeling in GREAPMC enables reliable reactor analysis while significantly improving geometry modeling flexibility. Although the CSG method enables exact modeling of complex non-fuel and ex-core geometries, it generally requires more simulation time than cell-based modeling due to cell search operations. Future work will focus on improving computational performance while maintaining modeling accuracy by introducing optimized cell search operations and combining CSG and cell-based approaches, where fuel regions are treated by the cell-based method, while complex structures by the CSG method.

ACKNOWLDEGEMETS

This work was supported by the National Research Foundation of Korea(NRF) grant funded by the Korea government(MSIT) (No. RS-2025-13222972).

REFERENCES

[1] M. R. Ali, M. S. Aygül and D. Lee, "Development of New GPU-Optimized Reactor Physics Monte Carlo Code GREAPMC,"*Nuclear Science and Engineering*, pp.1–16, 2025.
[2] Andrew T. Godfrey (2014) *VERA Core Physics Benchmark Progression Problem Specifications*, Revision 4, CASL-U-2012-0131-004, Oak Ridge National Laboratory, August 29, 2014.
[3] T. D. C. Nguyen, H. Lee, S. Choi and D. Lee, "Validation of UNIST Monte Carlo Code MCS Using VERA Progression Problems," *Nuclear Engineering and Technology*, vol. 52, no.5, pp.878–888, 2020.